

# Biosynthesis of Copper Oxide Nanoparticles with Potential Biomedical Applications

This article was published in the following Dove Press journal:  
International Journal of Nanomedicine

Navid Rabiee<sup>1</sup>  
Mojtaba Bagherzadeh<sup>1</sup>  
Mahsa Kiani<sup>1</sup>  
Amir Mohammad Ghadiri<sup>2</sup>  
Fatemeh Etessamifar<sup>1</sup>  
Amir Hossein Jaberizadeh<sup>2</sup>  
Alireza Shakeri<sup>2</sup>

<sup>1</sup>Department of Chemistry, Sharif University of Technology, Tehran 11155-3516, Iran; <sup>2</sup>School of Chemistry, College of Science, University of Tehran, Tehran, Iran

**Introduction:** In recent years, the use of cost-effective, multifunctional, environmentally friendly and simple prepared nanomaterials/nanoparticles have been emerged considerably. In this manner, different synthesizing methods were reported and optimized, but there is still lack of a comprehensive method with multifunctional properties.

**Materials and Methods:** In this study, we aim to synthesis the copper oxide nanoparticles using *Achillea millefolium* leaf extracts for the first time. Catalytic activity was investigated by in situ azide alkyne cycloaddition click and also  $A^3$  coupling reaction, and optimized in terms of temperature, solvent, and time of the reaction. Furthermore, the photocatalytic activity of the synthesized nanoparticles was screened in terms of degradation methylene blue dye. Biological activity of the synthesized nanoparticles was evaluated in terms of antibacterial and anti-fungal assessments against *Staphylococcus aureus*, *M. tuberculosis*, *E. coli*, *K. pneumoniae*, *P. mirabilis*, *C. diphtheriae* and *S. pyogenes* bacteria's and *G. albicans*, *A. flavus*, *M. canis* and *G. glabrata* fungus. In the next step, the biosynthesized CuO-NPs were screened by MTT and NTU assays.

**Results:** Based on our knowledge, this is a comprehensive study on the catalytic and biological activity of copper oxide nanoparticles synthesizing from *Achillea millefolium*, which presents great and significant results (in both catalytic and biological activities) based on a simple and green procedure.

**Conclusion:** Comprehensive biomedical and catalytic investigation of the biosynthesized CuO-NPs showed the mentioned method leads to synthesis of more eco-friendly nanoparticles. The in vitro studies showed promising and considerable results, and due to the great stability of these nanoparticles in a green media, effective biological activity considered as an advantageous.

**Keywords:** copper oxide nanoparticles, green synthesis, catalytic activity, antibacterial activity, antifungal activity

## Introduction

Nanotechnology, which is considered as a scientific revolution in the present century, is developing rapidly in several subjects including chemistry, physics, engineering and medicine. Nanotechnology plays a very important role in modern research; its high ability in many fields, such as pharmacy, electronics, health, food, biomedical sciences, pharmaceuticals, chemistry and chemical industry, energy sciences, cosmetics, environmental health, mechanics and space industry. Among these wide applications, using metal nanoparticles have found considerable results in several applications including nanochemistry. In the last years, there were a wide interest between scientists in utilizing the principles of green chemistry to synthesize metal nanoparticles for several applications. In this case, gold and silver nanoparticles synthesized from

Correspondence: Mojtaba Bagherzadeh  
Tel +98(21)66165301  
Email bagherzadeh@sharif.edu

vegetable oil can be used as anti-bacterial agents, and recent reports revealed that copper nanoparticles (with the band gap of about 2.43 eV) show considerable anti-bacterial, anti-fungal and related effects in comparison with bulk CuO (with the band gap of about 1.85 eV) which have been considered in this study. Green chemistry is the design, development and implementation of chemical products and processes to reduce or eliminate the use and generation of substances hazardous to human health and the environment. It should be noted that, strategies should be addressed environmental issues and related subjects, which in this case we have been pointed the use of biodegradable polymers, environmentally benign solvents and non-toxic chemicals.<sup>1-8</sup>

There are several steps that can be able to tune or optimize via green chemistry, however, in the synthesis of metal nanoparticles through preparing from corresponding metal ion salt by a reduction processes, three factors have been considered as an opportunity to implement green chemistry in this field. The first one is solvent, second is reducing agent and the last one is capping agent or dispersing agent. In this matter, green chemistry area focused on optimizing one of these factors via finding green alternatives for them, or using multicomponent as in situ alternatives for these three factors simultaneously.<sup>9-15</sup>

The use of metal nanoparticles has different applications in different industries, but in general, these nanoparticles play a very important role as catalysts for different reactions including Mizoroki-Heck, Sonogashira, A<sup>3</sup> and carbon-coupling reactions. One of the important factors that can increase the efficiency of different industries is the use of nanoparticles, or better to say, different catalysts with multiple functions, as well as low cost along with high life-time and high efficiency. Using synthetic methods of green chemistry can help to achieve these important parameters.<sup>16-20</sup>

In the present study, we have been focused on synthesizing and characterizing copper oxide nanoparticles from *Achillea millefolium*, and investigating potential biological and catalytic activities of these nanoparticles. Full investigation in terms of biological activities from antibacterial and antifungal towards cellular toxicity assessments were accomplished with details.

## Materials and Methods

### Chemicals, Reagents and Plant Source

All of the materials and reagents were of analytical grade and obtained from Sigma-Aldrich, Germany. *Achillea millefolium* leaves were collected from

Kurdistan, Iran. The plant, *Achillea millefolium*, was previously identified in the literature by GC-MS technique, therefore, we use the fact that have been published for the concept of this study.<sup>21-23</sup>

### Preparation of Plant Extract for Synthesis of Nanoparticles

Preparation of the plant extract for the synthesis of nanoparticles were performed based on the literature.<sup>24</sup> Briefly, the plant, *Achillea millefolium*, collected from the nature, and washed for several times with deionized water, and after that prepared for drying at room temperature. The dried ones were poured into mortar and turn into the fine powder. The fine powders were dispersed in deionized water (150 mL) and heated up to 70°C for about 30 minutes. The resulted suspension, or in some cases fine solution, were filtered through a filter paper and the obtained extract was stored at 4°C for further procedures. Based on the literature, the extraction yield is not an important parameter for this type of studies,<sup>25,26</sup> but by using spectroscopy techniques, the extraction yield was determined and calculated about 60% which is appropriate for our study.

### Synthesizing of Copper Oxide Nanoparticles

To achieve these nanoparticles from the *Achillea millefolium* leaf broth, 40 mL of *Achillea millefolium* was poured into 100 mL of the cupric sulfate solution (1 mM) and the suspension was stirred for a day at room temperature. After that, the synthesized nanoparticles were filtered and centrifuged at 10,000 rpm for about 30 minutes. In this method, the leaf extract was act as both reducing agent and stabilizing agent, which help the growth of the nanoparticles and also reduce and minimize the aggregation process of the nanoparticles by capping them with aldehyde and ketone groups.

As purification of the synthesized nanoparticles is an important procedure in nanoparticle synthesis, the exact procedure for nanoparticle separations explained there. Briefly, to approach this goal, separation of the unreacted components from the synthesized CuO-NPs, the mixture was centrifuged at 15,000 rpm for 15 minutes and washed several times using deionized water. Freeze-drying was applied to obtain dried powder of the CuO-NPs. In addition, the separations based on chromatographic techniques including ion-exchange chromatography and was

also used. The yield of synthesis of the CuO-NPs was calculated 88%, which is appropriate for this type of studies and is above the chemical and physical synthesis methods.<sup>27–29</sup>

## Characterization of Synthesized Nanoparticles

Characterization techniques were applied same as our previous publication.<sup>30</sup> UV–vis spectrometer (Perkin Elmer Lambda 25) was applied to record absorbance of CuO-NPs in the range of 200–800 nm. Fourier transformed infrared spectroscopy (FT-IR) spectrum was applied using JASCO FT-IR-460 spectrometer in the range of 400–4000  $\text{cm}^{-1}$ . Powdered X-ray diffraction (PXRD) spectra were obtained by an automated Philips X'Pert X-ray diffractometer with Cu Ka radiation (40 kV and 30 mA) for  $2\theta$  values over the range of 10–80. The morphology of synthesized CuO-NPs was observed by field emission scanning electron microscope (FESEM, TESCAN MIRA-3) under an acceleration voltage of 30–250 kV.

## General Catalytic Procedure

In this step, which have been adopted from our recent publication,<sup>31</sup> CuO nanoparticles (as a catalyst) were added to the reactor containing 0.5 mmol alkyne, 0.55 mmol  $\text{NaN}_3$ , 0.55 mmol the organic halide and 2 mL of water. This mixture was stirred at 70°C for 10 hours and the reaction monitored by thin-layer chromatography (TLC). After that, 5 mL of water was added dropwise to the final solution and the final product was extracted from the aqueous phase with ethyl acetate. The organic layer was dried with anhydrous  $\text{CaCl}_2$  and the solvent was removed under reduced pressure to give the corresponding 1,2,3-triazoles. After extraction with ethyl acetate, the reaction mixture was filtered and the residue was subjected to column chromatography (eluent, 40% EtOAc in n-hexane).

Based on the literature,<sup>32–34</sup> there is a typical procedure for the synthesis of propargylamine derivatives via  $\text{A}^3$  coupling reaction, briefly, 0.5 mmol of secondary amine and 0.5 mmol of aldehyde along with 0.55 mmol alkyne were reacted in the presence of suitable solvent and the catalyst, in this case CuO-NPs, at the precision temperature and time. It should be mentioned that the progress of the reaction was screened by TLC.

## Photocatalytic Activity

In this step, the photocatalytic activities of the CuO-NPs were evaluated based on the literature<sup>35</sup> by calculating the MB degradation in an aqueous solution (a visible light irradiation with the wavelength of  $\lambda > 420$  nm was applied). For this purpose, a lamp (mercury one, with the precision power (A 250-W)) as the source of light was used. To determine the photocatalytic activity of the CuO-NPs, an optical glass with around 400 to 800 nm cutoff filter was applied. For each experiment, the process (photocatalytic experiment) was conducted with a photoreactor (usually 100 mL one) at ambient temperature. To conduct each analysis, a precise amount of the CuO-NPs as the photocatalyst ( $0.2 \text{ g L}^{-1}$ ) was dispersed (with the aims of the ultrasonic) in a precision concentration of aqueous solution of MB ( $8 \text{ mg L}^{-1}$ ) and the solution was exposed to the irradiation under mild stirring. After the exact time interval (with the regular steps), 5 mL of the exposed solution was separated and was screened at the absorbance wavelength of 660 nm to calculate the concentration of MB.

## Antibacterial Activity

To investigate the potential antibacterial activity, disc diffusion technique was applied based on the literature.<sup>36–38</sup> These strains of bacteria are stable in nutrient broth for a day at 37°C. In the following, they were streaked over surface of the Muller Hinton Agar using the sterile cotton swabs.

The obtained were used extract against the broth inoculums (czapek Dox) with the age of about a day that have been cultured on the agar plate for different gram-positive and gram-negative spores. In the following, the synthesized nanoparticles and also the standard solution were dissolved in DMSO, and four well plates on the Hinton agar were used for the procedure. Then 15  $\mu\text{L}$  of compound was injected on the paper disc (in sterile form), after that the extract was kept for several minutes to dry meanwhile and the disc kept on the plate surface. In the next step, the plates are incubated for at 37°C for a day and the antibacterial activities were calculated as diameter zone of inhibitive.

## Anti-Fungal Activity

In this stage, the CuO-NPs were investigated for the potential antifungal activity against different kind of fungi's. For this purpose, a culture including sabouraud dextrose agar (Sigma-Aldrich GmbH, Germany) ( $10^6$

cfu/mL) transferred to a plates and the prepared discs were exposed to the exact concentration of the synthesized nanoparticles and finally were stabilized on the surface of the agar. After that, the plates were incubated for a week at 32°C. To acquire the results, inhibition zones were recorded in mm in comparison with the standard drugs, amphotericin B and miconazole.

## Cell Culture

In this study, HepG2 (ATCC HB-8065<sup>TM</sup>) cells were applied in all of the following experiments. HepG2 cells were grown in DMEM (Gibco, Invitrogen, Norway), which have been supplemented with 1 mM amino acids (non-essential one's), 1.5 g/L sodium bicarbonate and fetal bovine serum (10%) (FBS) and 5% CO<sub>2</sub> at 37°C. In the next step, at about 85% confluence, 0.25% of trypsin was applied for harvesting the cells and also were cultured into a flask. The cells with the nanoparticles were diluted with exact amounts, and sonicated for about 15 minutes to avoid the aggregations. It should be mentioned that the concentrations were achieved by dose-response study (data not shown), and in some circumstances, the HepG2 cells were exposed to N-acetyl-cysteine (10 mM) for about 1.5 hours before treatment by the CuO-NPs. For this study, the synthesized nanoparticles and the leaf extract solutions were dispersed in the culture medium (final volume should be 0.2% in maximum), the treatment was performed for 12 hours, and after that, the cells were washed by PBS.

## Colorimetric Cell Viability Assay

To investigate the cytotoxicity of the prepared synthesized nanoparticles and also the cellular proliferation of them, HepG2 cell line was applied based on the protocol was mentioned in the literature.<sup>39–42</sup> Briefly, the mentioned cells were seeded in a 96-well plate tissue culture at a standard density (10<sup>4</sup> cells per well) and incubated in 100 µL of DMEM/F12 which have been supplemented with 10% FBS for a day. Afterward, the culture media were replaced with the fresh one containing several dilutions of the synthesized material, and the prepared cells were incubated for 5 hours. In the following, the resulted media were replaced with 100 µL of the fresh one for additional 24 hours. Finally, the medium was replaced with 100 µL of the fresh one including MTT, and were also incubated again at 37°C for 4 hours. After successful incubation for 4 hours, the resulted medium was aspirated and the MTT

formazan which have been generated in this step was dissolved in the next 100 µL of DMSO and the absorbance of each well was recorded utilizing a microplate reader (570 nm). The resulted data are presented as average ± SD (n=3).

## Neutral Red Uptake Assay

In this step, the neutral red uptake (NRU) assay was investigated based on the literature with some modifications. Briefly, about 10<sup>4</sup> cells/well were cultured in a 96-well plates and after that, exposed to the different CuO-NPs concentration solutions for a day. After 24 hours, the solutions were aspirated carefully and the obtained cells were washed for several times with PBS and incubated for about 4 hours at the medium (including 60 µg/mL of neutral red). The final medium was washed carefully with a solution of calcium chloride (1%) and formaldehyde (0.5%), and the cells were incubated again for 30 minutes at the same condition, in a mixture of ethanol (50%) and acetic acid (1%). In the final step, 100 µL of the supernatant was transferred to a plate and the absorbance measured at 540 nm by microplate reader. The resulted data are presented as average ± SD (n=3).

## Statistical Analysis

All of the statistical analysis related to MTT assays and other experiments were performed by one-way analysis of variance (ANOVA) followed by OriginPro 9.1 software compatible tests of Bonferroni *post-hoc*. In addition, all data represent means of ±SD of at least n=3 independent sets of experiments.

## Results and Discussion

### FTIR Results

Based on the FTIR spectrum in Figure 1, the semi-broad band observed at around 3408 cm<sup>-1</sup> illustrate the stretching frequency of hydroxyl group, which is an indicator of the surface morphology of the synthesized nanoparticles. Furthermore, a peak at 1056 cm<sup>-1</sup> corresponds to the ester bonds between copper species and also hydroxyl groups. Finally, the obtained spectrum was compared to the prestigious papers in the literature and confirmed successful biosynthesis of the CuO-NPs.<sup>43–45</sup>

### UV-Vis Spectra Analysis

The absorption spectra (Figure 2) represented a peak at around 250 nm that is an index of Cu<sub>2</sub>O phases.<sup>46</sup> And

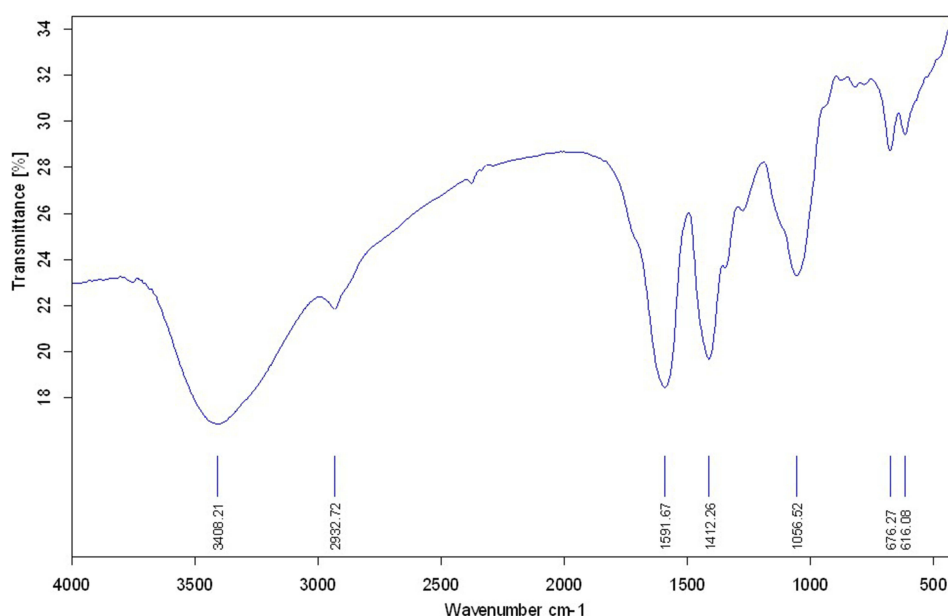


**Figure 1** The FT-IR spectra of synthesized CuO-NPs.

another peak at around 365 nm represent correct bio-synthesized of copper oxide nanoparticles.<sup>47–49</sup> It should be mentioned that, the broadness of the absorption peak is because of wide size distribution of these nanoparticles.

## FESEM Analysis

To evaluate the morphology of synthesized nanoparticles, FESEM analysis was used. FESEM images of the synthesized copper oxide nanoparticles using *Achillea millefolium* is shown in Figure 3. The biosynthesized

CuO-NPs by this method reveals a monodispersed distribution with also homogenous size range. The average particle size of the CuO nanoparticles is around 28 nm. The shape and morphology of the nanoparticles are dependent on the reducing agent as well as stabilizing agent, which in this case, both of them are the plant extract, therefore, the semi-spherical morphology of them are because of the good candidate that is chosen in this study. These data are in full agreement with recent prestigious studies around biosynthesizing CuO-NPs.<sup>50–52</sup>

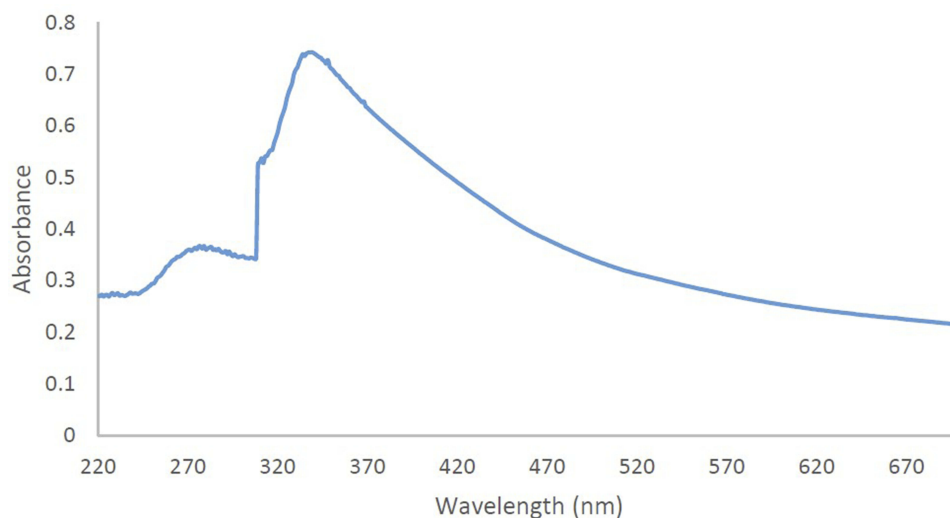


**Figure 2** UV/Vis spectrum of the synthesized CuO-NPs.



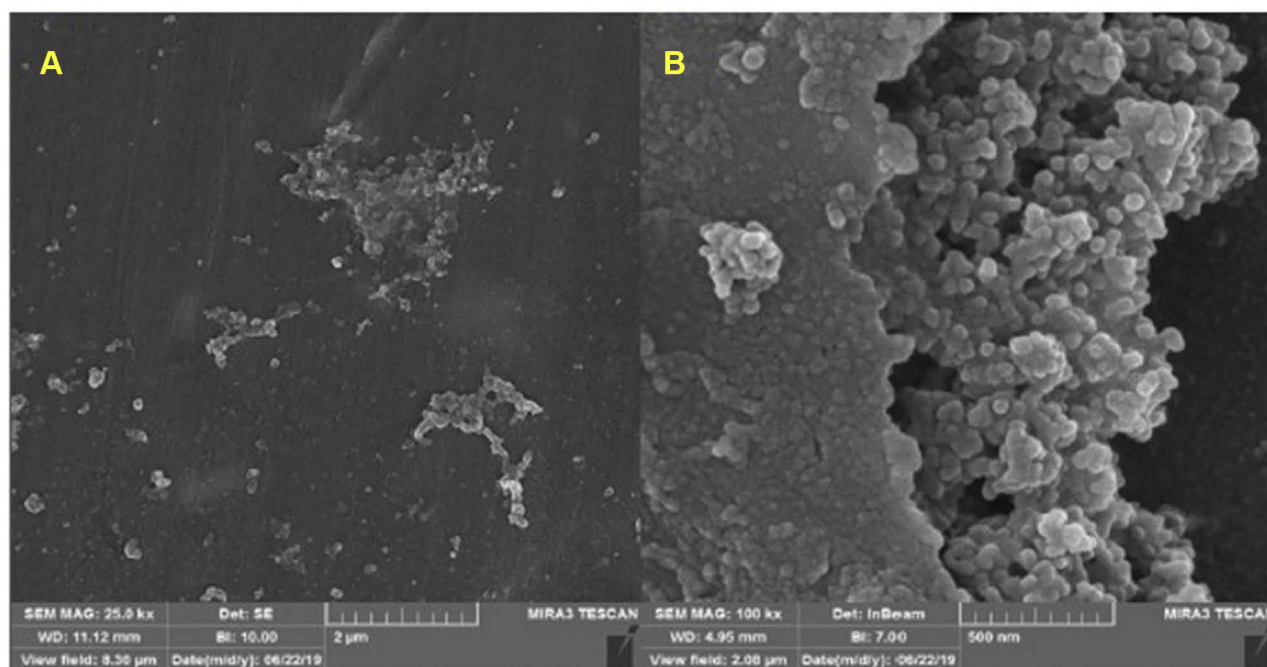


**Figure 3** FESEM images of the synthesized CuO-NPs with different magnifications: (A) 2  $\mu$ m and (B) 500 nm.

## XRD Analysis

PXRD was used to assess the exact structural chemistry of CuO-NPs (Figure 4). There are three main characteristic diffraction peaks for Cu are at around  $2\theta = 43^\circ$ ,  $50^\circ$ ,  $74^\circ$  which correspond to the (111), (200), (220) crystallographic planes of face-centered cubic (fcc) Cu phase (JCPDS card No. 04-0784). And a diffraction peak around  $29^\circ$  indicates the (110) crystallographic plane of  $\text{Cu}_2\text{O}$ . In addition, diffraction peak at around  $2\theta = 38^\circ$  correspond to the (111) crystallographic plane of  $\text{Cu}_2\text{O}$ .

These diffraction peaks are in good agreement with the literature.<sup>53–55</sup>

## Catalytic Activity

To investigate the catalytic activity of the synthesized nanoparticles, a typical reaction between sodium azide, benzyl chloride and phenyl acetylene were carried out. In order to obtain an optimized condition, this reaction optimized in terms of reaction time, amount of catalyst, solvent and reaction temperature and these results shown in

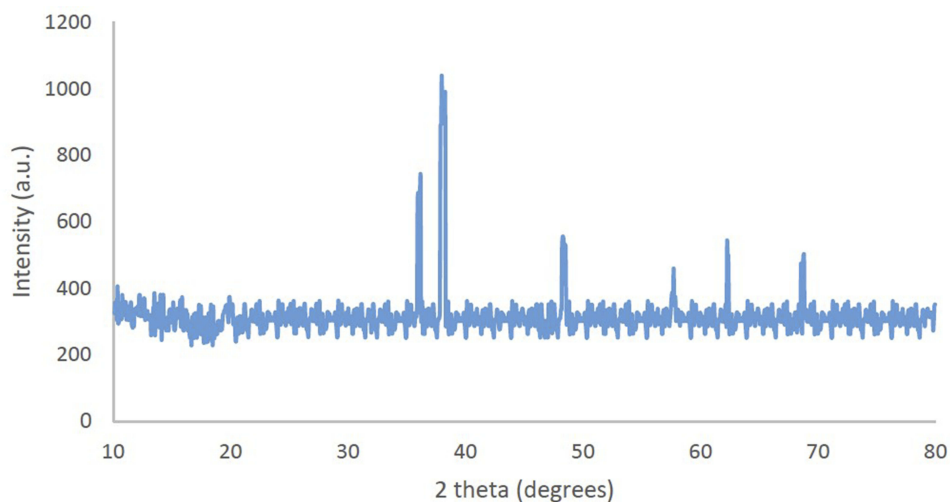


**Figure 4** XRD of the synthesized CuO-NPs.

**Table 1** The Effect of Time, Temperature and the Amount of Catalyst on the Cycloaddition of Benzyl Chloride with Phenyl Acetylene in the Presence of Sodium Azide.<sup>a</sup>

Entry	Cat (mol %)	Temp (°C)	Time (h)	Yield (%) <sup>b</sup>
1	—	70	12	0
2	0.27	70	6	79
3	0.54	70	6	81
4	0.81	70	6	88
5	1.08	70	6	92
6	1.35	70	6	98
7	1.62	70	6	98
9	1.35	40	6	68
10	1.35	50	6	79
11	1.35	60	6	89
12	1.35	70	4	66
13	1.35	70	2	55

**Notes:** <sup>a</sup>Reaction conditions: 0.5 mmol of phenylacetylene, 0.55 mmol of benzyl chloride, 0.55 mmol of sodium azide, 2 mL of H<sub>2</sub>O. <sup>b</sup>Isolated yields.

**Table 1.** In the first step, no catalyst was used, and no product observed (entries 1, [Table 1](#)), however, in the presence of catalyst, a considerable increase in yield was monitored, to be exact, by loading of the 0.27 to 1.35 mol % (entries 2 and 6, [Table 1](#), respectively) of the catalyst, the yield increased sharply from 79% to 98%, and further increase in the amount of the loaded catalyst (entry 7, [Table 1](#)) showed no further increase in the isolated yield. From another perspective, different solvents were used to optimize the condition. Interestingly, for this cycloaddition reaction, organic solvents (acetone, chloroform, toluene

and ethanol) showed poor yield and by using water as the solvent, the best results were obtained ([Figure 5](#)). In addition, an acceptable reactivity was screened when the reaction mixture was heated to 70°C (entries 9, 10 and 11, [Table 1](#)). Another interesting results were of optimizing the time of the reaction, which in this case by increasing the time of the reaction two folds from 2 to 4 hours, isolated yield gradually increased (entries 12 and 13, [Table 1](#)). In addition, different substituted groups were investigated as well. In this regard, different substituted phenyl acetylenes and benzyl halides were used with the optimized condition to produce the isolated product ([Table 2](#)). Generally, the results showed that by using electron donating or electron-withdrawing groups on the phenyl acetylenes and benzyl halides, no significant changes in isolated yield were screened, however, steric hindrance has effect on the isolated yield, to be exact, *p*-methyl benzyl chloride is more reactive than *o*-methyl benzyl chloride because of the less steric hindrance.<sup>56</sup> The results showed that benzyl chloride is more reactive than benzyl bromide, and it was predicted.<sup>31</sup> For further investigation, 2-methyl-3-butyne-2-ol and propargyl alcohol were used as a terminal alkyne and the reaction accomplished smoothly to the final product in the moderated yields.

In the final step, a logical comparison based on the optimized condition as well as isolated yield were made between this work and the literature ([Table 3](#)). The present work revealed an acceptable and promising

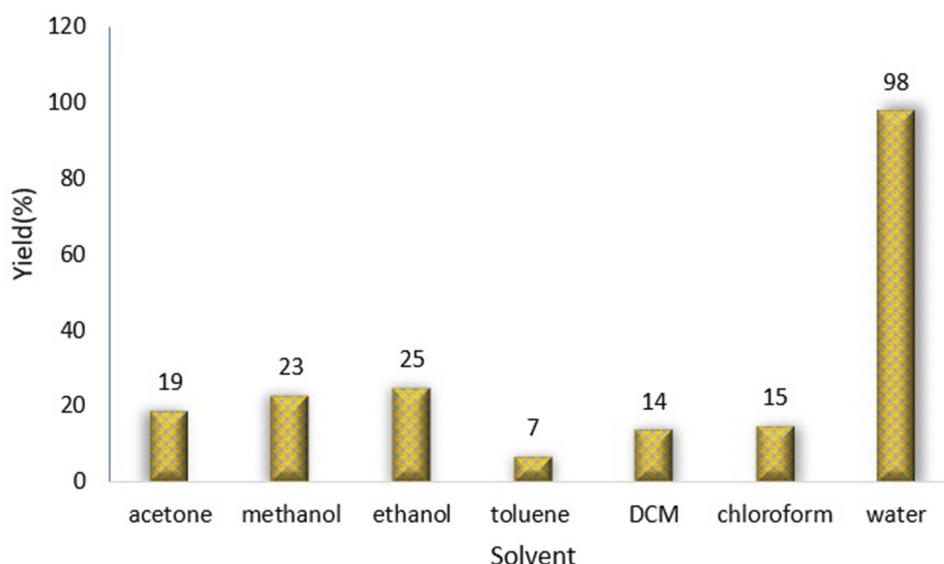


**Figure 5** Effect of solvent on the cycloaddition of benzyl chloride with phenyl acetylene and sodium azide. Reaction condition: 0.5 mmol of phenylacetylene, 0.55 mmol of benzyl chloride, 0.55 mmol of sodium azide, solvent 2 mL, 70°C, 6h. Isolated yields.

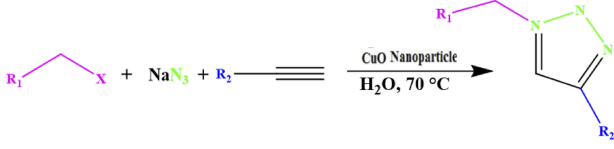
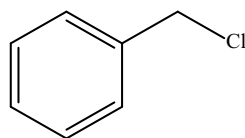
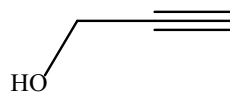
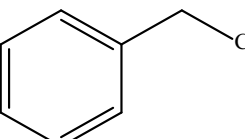
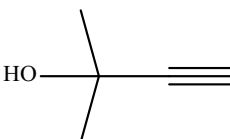
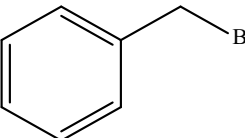
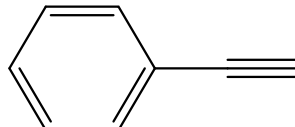
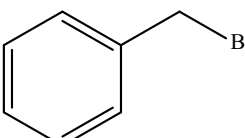
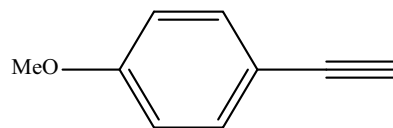
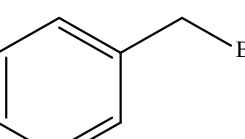
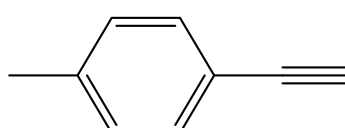
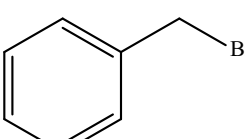
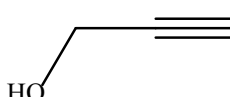
**Table 2** Cycloaddition of Alkyl Halides with Terminal Alkynes in the Presence of CuO Catalysts and NaN<sub>3</sub> Under the Optimized Reaction Conditions.<sup>a</sup>

Entry	Aliphatic halide	Alkyne	Yield(%) <sup>b</sup>	
1			98	
2			89	
3			95	
4			94	
5			97	
6			95	

(Continued)

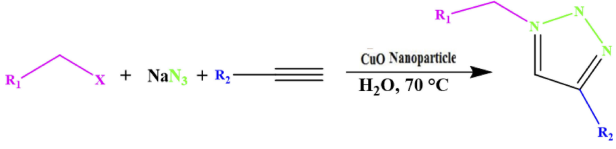
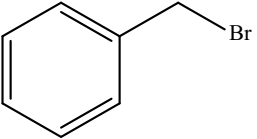
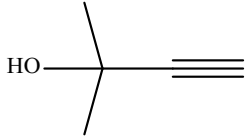


Table 2 (Continued).

			
Entry	Aliphatic halide	Alkyne	Yield(%) <sup>b</sup>
7			68
8			61
9			81
10			91
11			88
12			62

(Continued)

**Table 2** (Continued).

			
Entry	Aliphatic halide	Alkyne	Yield(%) <sup>b</sup>
13			58

**Notes:** <sup>a</sup>Reaction conditions: 0.5 mmol of terminal alkyne, 0.55 mmol of alkyl halide, 0.55 mmol of sodium azide, 2 mL of H<sub>2</sub>O, 70 °C and 6 h. <sup>b</sup>Isolated yields.

**Table 3** Recently Reported Catalytic Systems for AAC in the Presence of CuO Nanoparticle

Entry	Catalyst	Conditions	Yield (%)	Ref.
1	Cu(NO <sub>3</sub> ) <sub>2</sub> · 3H <sub>2</sub> O	Catalyst (20 mol%)/H <sub>2</sub> O/20 h/r.t.	13	57
2	Cu(OAc) <sub>2</sub> · H <sub>2</sub> O	Catalyst (20 mol%)/H <sub>2</sub> O/20 h/r.t.	77	57
3	Cu NPs/silica coated maghemite	Catalyst (4.3 mol%)/H <sub>2</sub> O/2h/70 °C	83	58
4	CuO nanowires	Catalyst (5.0 mol%)/H <sub>2</sub> O: t-BuOH/12h/r. t.	99	59
5	Cu@Cu <sub>2</sub> O core-shell nanocatalyst	Catalyst (2.3 mol%)/H <sub>2</sub> O: t-BuOH/5h/50 °C	99	60
6	Cu(II)-MOF	Catalyst (2.3 mol%)/H <sub>2</sub> O: t-BuOH/5h/50 °C	12	60
7	CuO nanoparticle	Catalyst (1.3 mol%)/H <sub>2</sub> O/6h/70 °C	98	Present work

results without using inert atmosphere and sodium ascorbate, however, the other publications showed that they are necessary. In addition, in the present work, the crucial factors such as temperature, reaction time and amount of the catalyst were optimized and based on the recent publications, the present catalyst accomplished the reaction in lower temperature, less reaction time and less amount of the catalyst in comparison with the other studies. It should be mentioned that, in situ generation of organic azides by a simple procedure and green catalyst can be considered as one of the advantages of this work.

To investigate the catalytic activity of the synthesized nanoparticles, a typical reaction between an aldehyde, amine and alkyne was carried out. To obtain the optimum conditions, initially the solvent was optimized (Table 4), and based on the results, chloroform was found to be the optimum solvent for this typical reaction (mechanism Figure 6). Furthermore, the time of the reaction was optimized in the absence of catalyst

and also in the presence of the precision amount of the catalyst (Table 5), and 20 hours found to be the optimized time reaction in the chloroform as the solvent. In the next step, the amount of the catalyst was optimized (Table 6) and 0.01 g was found to be the optimum amount of catalyst in this typical reaction. And in the final step of the investigation based on the A<sup>3</sup> coupling

**Table 4** The Effect of Solvent, on the A<sup>3</sup> Coupling Reaction on the Reflux Temperature Zone

Entry	Cat (mol %)	Solvent	Time (h)	Yield (%)
1	–	Water	24	8
2	0.003	Water	24	15
3	–	Toluene	24	54
4	0.003	Toluene	24	66
5	–	Chloroform	24	69
6	0.003	Chloroform	24	77
7	–	Acetonitrile	24	Trace
9	0.003	Acetonitrile	24	Trace

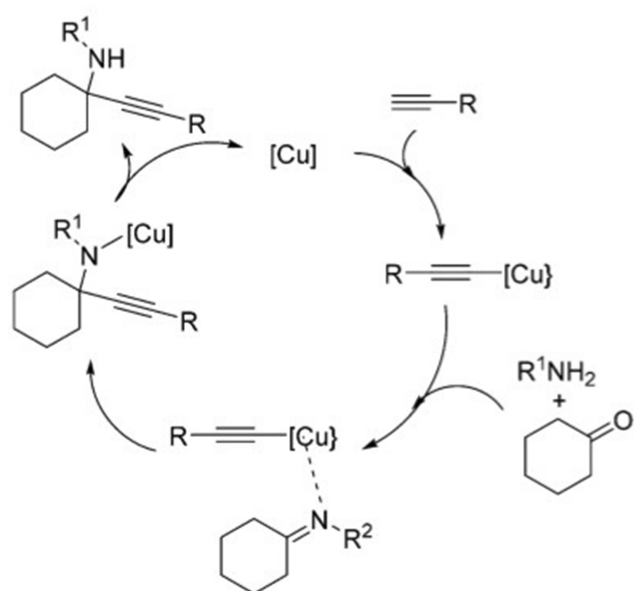


**Figure 6** Catalytic mechanism of the A<sup>3</sup> coupling reaction.

reaction, different derivatives of the precursors were screened based on the optimum condition (Table 7).

## Antibacterial Activity

The synthesized copper oxide nanoparticle from *Achillea millefolium* screened in vitro antibacterial activity against seven different bacteria's, *Staphylococcus aureus*, *M. tuberculosis*, *E. coli*, *K. pneumoniae*, *P. mirabili*, *C. diphtheriae* and *S. pyogenes* according to the literature and result that compared to the Imipenem standard drug shown in Table 8. Based on the results, the biosynthesized CuO-NPs with low concentrations are really competitive in terms of their antibacterial activity with the mentioned standard drug, but, there is a interesting results in different concentration of the biosynthesized nanoparticles, to be exact, by increasing the concentration of the nanoparticles, the potential antibacterial activity of the biosynthesized CuO-NPs against six

**Table 5** The Effect of Time, on the A<sup>3</sup> Coupling Reaction on the Chloroform as the Solvent

Entry	Cat (mol %)	Temperature	Time (h)	Yield (%)
1	–	Reflux	18	68
2	0.003	Reflux	18	77
3	–	Reflux	20	81
4	0.003	Reflux	20	88.5
5	–	Reflux	24	86
6	0.003	Reflux	24	91

**Table 6** The Effect of Catalyst Amount, on the A<sup>3</sup> Coupling Reaction on the Chloroform as the Solvent

Entry	Cat (mol %)	Temperature	Time (h)	Yield (%)
1	0.003	Reflux	20	79
2	0.005	Reflux	20	82
3	0.01	Reflux	20	94

different bacterial increased significantly, but against another bacteria increase in a gradual step. The mechanism of the antibacterial properties of the biosynthesized metal oxide nanoparticles have been proved in several prestigious papers, that is based on the strong interaction between the bacteria's cell wall and the metal ions, which resulted in rupturing the cell walls.<sup>61–67</sup>

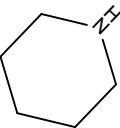
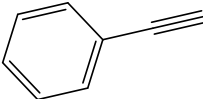
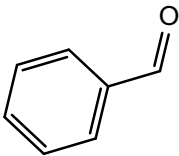
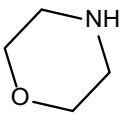
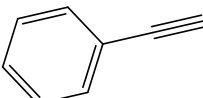
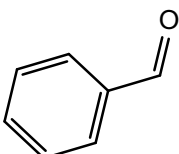
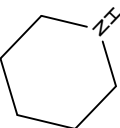
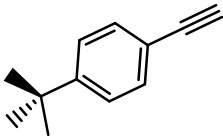
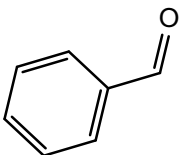
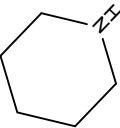
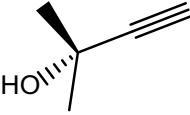
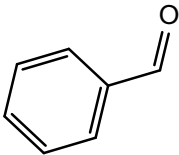
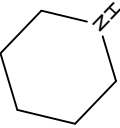
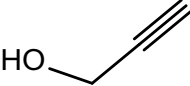
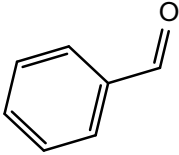
## Anti-Fungal Activity

The synthesized copper oxide nanoparticle from *Achillea millefolium* screened in vitro anti-fungal activity against four different fungus, *G. Albicans*, *A. flavus*, *M. canis* and *G. glabrata* according to the literature and result that compared to the Amphotericin B and Miconazole standard drugs shown in Table 9. Based on the results, the biosynthesized CuO-NPs have effective antifungal activity against different fungus, which could be because of entering the CuO-NPs to the cell membranes and in the following leads to cease the cells divisions via strong interaction on the respiratory chains, however, to date, this is the first report of the potential antifungal activity of CuO-NPs like this, and this report is really important to show the effect of the biosynthesis method to enhance and improve the potential antibacterial as well as anti-fungal activity in metal oxide nanoparticles.<sup>68–71</sup>

## Photocatalytic Activity

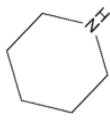
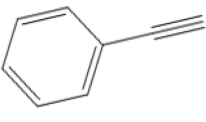
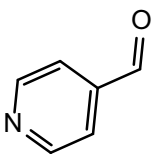
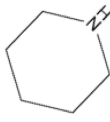
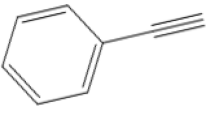
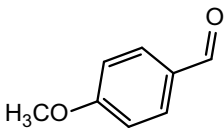
To investigate the photocatalytic activity of the synthesized CuO-NPs, MB was chosen in the dye degradation process, and the UV-Vis spectrum with the maximum absorption of 660 nm was applied. The solution containing the dye with both NPs were irradiated by visible light and degradation of the dye was screened by UV-Vis spectrum and the spectra taken at different times of irradiation are represented in Figure 7. Based on the results, there is considerable decrease in the maximum absorbance in the presence of the irradiation and MB was nearly degraded after about 100 minutes and in the following the full degradation of the MB was observed after 120 minutes in the presence of CuO-NPs which it

**Table 7** The Performance of the CuO-NPs as the Catalyst in the Typical A3 Coupling Reaction in the Presence of Different Derivatives of the Precursors

$R^1-C\equiv C + R^2CHO + R^3NHR^4 \xrightarrow{\text{catalyst}} R^1-C\equiv C-CH(R^2)-CH_2-NR^3R^4$				
Entry	Amine	Alkyne	Aldehyde	Yield (%)
1				94
2				100
3				82
4				61
5				74

(Continued)

**Table 7** (Continued).

$R^1-C\equiv C + R^2CHO + R^3NHR^4 \xrightarrow{\text{catalyst}} R^1-C\equiv C-CH(R^2)-CH_2-NR^3R^4$				
Entry	Amine	Alkyne	Aldehyde	Yield (%)
6				14
7				85

**Table 8** Antibacterial Activity of Copper Oxide Nanoparticles

Concentration of NPs	<i>Staphylococcus aureus</i>	<i>M. tuberculosis</i>	<i>E. coli</i>	<i>K. pneumoniae</i>	<i>P. mirabili</i>	<i>C. diphtheriae</i>	<i>S. pyogenes</i>
Based on zone of inhibition (mm) <sup>a</sup>							
10 µg/mL	12.8 ± 0.5	29.1 ± 1.2	23.3 ± 0.9	18.5 ± 0.8	19.4 ± 0.6	27.1 ± 1.0	11.6 ± 0.4
50 µg/mL	26.1 ± 1.1	37.1 ± 1.5	28.3 ± 1.1	29.3 ± 1.6	25.2 ± 1.1	24.7 ± 1.0	17.2 ± 0.8
100 µg/mL	30.3 ± 1.3	54 ± 1.9	36.2 ± 1.7	30.5 ± 1.5	34.7 ± 1.8	35.8 ± 2.0	22.5 ± 1.1
Imipenem Standard Drug	29 ± 1.2	30 ± 1.2	30 ± 1.2	25 ± 1.1	30 ± 1.2	30 ± 1.2	32 ± 1.2

**Notes:** <sup>a</sup>The data indicate the zone of inhibition of bacteria colonization for 24 hours and is presented as the mean (±SD) from three independent experiments, each comprising three microcultures per concentration level.

shows that CuO-NPs degraded a certain amount of color in acceptable time. The dye degradation mechanism based on the synthesized nanoparticles is based on producing the electron and holes after exposure to the irradiation, and by the reaction of electron with hydroxyl radicals, to be exact oxygen radicals, superoxide radicals were produced, and the oxygen radicals could be able to degrade the MB.

## Cell Viability Assays

For this purpose, the synthesized nanoparticles with the exact concentration were treated with HepG2 cells for about 24 hours and the cytotoxicity of them were

examined by both NRU and MTT assays (Figure 8). Based on the results, the green synthesized CuO-NPs considerable decreased the relative cell viability (in dose-dependent manner), and the decreasing trend is almost same in both MTT and NRU assays. It should be mentioned that, based on the prestigious papers in the literature, is the studies like that there is no evidence of effecting Cu<sup>2+</sup> release in the toxicity of the synthesized nanoparticles on HepG2 cells.<sup>39,72-74</sup>

## Conclusion

The present study deals with biosynthesis of CuO-NPs from *Achillea millefolium* leaves extracts, for the first



**Table 9** Antifungal Activity of Copper Oxide Nanoparticles

Concentration of NPs	<i>G. albicans</i>	<i>A. flavus</i>	<i>M. canis</i>	<i>G. glabrata</i>
Based on zone of inhibition (mm) <sup>a</sup>				
10 µg/mL	11.6 ± 0.5	12.1 ± 0.6	17.4 ± 0.9	15.2 ± 1.4
50 µg/mL	19.5 ± 0.6	20.3 ± 1.1	21.6 ± 1.5	18.6 ± 1.2
100 µg/mL	34.2 ± 1.4	31.8 ± 1.7	37.6 ± 2.1	23.7 ± 1.5
Miconazole	20 ± 0.9	25 ± 1.7	25 ± 1.9	25 ± 1.1
Amphotericin B	25 ± 1.1	30 ± 1.6	25 ± 1.9	30 ± 2.2

**Notes:** <sup>a</sup>The data indicate the zone of inhibition of bacteria colonization for 24 hours and is presented as the mean (±SD) from three independent experiments, each comprising three microcultures per concentration level.

time, and conducting a comprehensive study about both potential biological and catalytic activities. The results of catalytic activity of in situ azide-alkyne

cycloaddition click reaction, were of great importance and the best results were found in a green media (water) without any additional reagents, which make

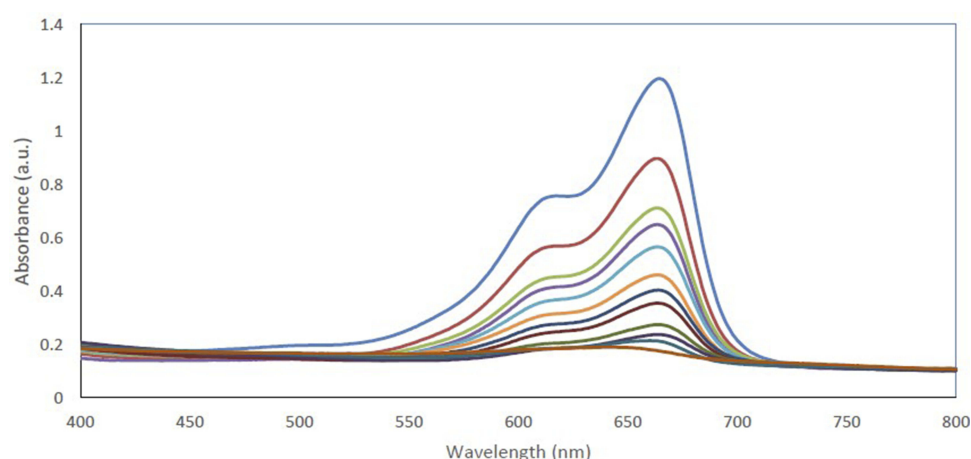


**Figure 7** The absorbance spectra of the MB dye in the presence of CuO-NPs in a typical photocatalytic degradation process. The results indicate the MB dye degradation in the presence of different light exposure is presented as a mean (±SD) from three independent experiments.

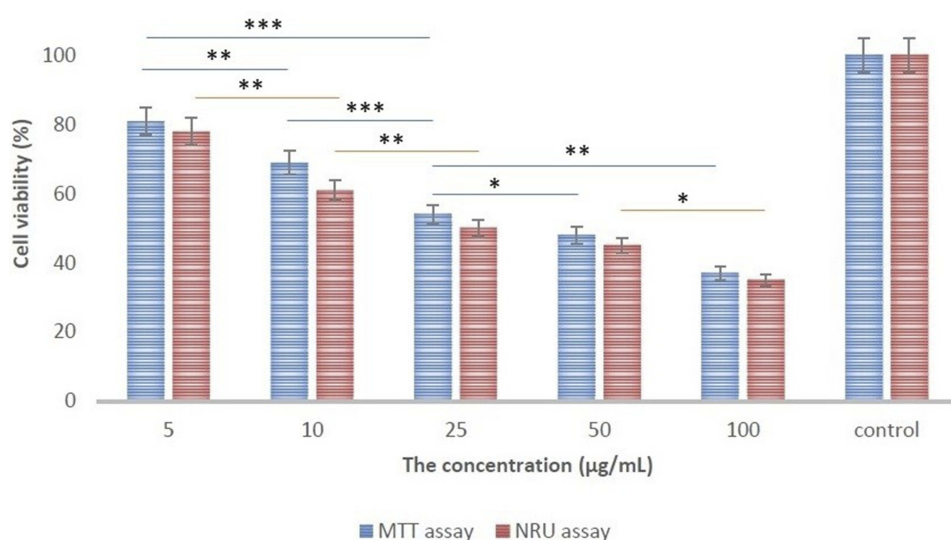


**Figure 8** The results of MTT and NRU assays. The data value indicates the MTT and NRU assays that results for each concentration is presented as a mean (±SD) from three independent experiments. \*  $p < 0.05$ , \*\*  $p < 0.01$  and \*\*\*  $p < 0.001$  indicates the meaningful values.

an emphasis on the potential of using these nanoparticles and this procedure in the industrial phase. In addition, the results of A<sup>3</sup> coupling reaction and also photocatalytic activities against MB dye was found to be very interesting. From another perspective, potential antibacterial and antifungal activity of these biosynthesized nanoparticles were screened against *Staphylococcus aureus*, *M. tuberculosis*, *E. coli*, *K. pneumoniae*, *P. mirabili*, *C. diphtheriae* and *S. pyogenes* bacteria's and *G. albicans*, *A. flavus*, *M. canis* and *G. glabrata* fungus and the results are considered as the synthesis method dependent of the metal oxide nanoparticles and also the first CuO-NPs with these considerable potential. In addition, comprehensive cellular investigation of the toxicity of the biosynthesized CuO-NPs showed the mentioned method leads to synthesis of more eco-friendly nanoparticles. The in vitro studies showed promising and considerable results, and due to the great stability of these nanoparticles in a green media, effective biological activity considered as an advantageous.

## Acknowledgments

Support of this work by the Sharif University of Technology Research Council is gratefully acknowledged.

## Disclosure

The authors report no conflicts of interest in this work.

## References

- Iravani S. Green synthesis of metal nanoparticles using plants. *Green Chem.* 2011;13(10):2638–2650. doi:10.1039/c1gc15386b
- Kalidindi SB, Jagirdar BR. Nanocatalysis and prospects of green chemistry. *ChemSusChem.* 2012;5(1):65–75. doi:10.1002/cssc.201100377
- Wu C, Mosher BP, Zeng T. One-step green route to narrowly dispersed copper nanocrystals. *J Nanopart Res.* 2006;8(6):965–969. doi:10.1007/s11051-005-9065-2
- Ghasemi A, Rabiee N, Ahmadi S, et al. Optical assays based on colloidal inorganic nanoparticles. *Analyst.* 2018;143(14):3249–3283.
- Nasab SG, Yazd MJ, Semnani A, et al. Natural corrosion inhibitors. *Synth Lect Biomed Eng.* 2019;14(1):1–96. doi:10.2200/S00910ED1V01Y201903MEC018
- Díaz-Requejo MM, Pérez PJ. Copper, silver and gold-based catalysts for carbene addition or insertion reactions. *J Organomet Chem.* 2005;690(24–25):5441–5450. doi:10.1016/j.jorganchem.2005.07.092
- Mishra A, Mehta A, Basu S, et al. Graphitic carbon nitride (g-C<sub>3</sub>N<sub>4</sub>)-based metal-free photocatalysts for water splitting: a review. *Carbon.* 2019;149:693–721. doi:10.1016/j.carbon.2019.04.104
- Wang H, Xu J-Z, Zhu J-J, et al. Preparation of CuO nanoparticles by microwave irradiation. *J Cryst Growth.* 2002;244(1):88–94. doi:10.1016/S0022-0248(02)01571-3
- Raveendran P, Fu J, Wallen SL. Completely “green” synthesis and stabilization of metal nanoparticles. *J Am Chem Soc.* 2003;125(46):13940–13941. doi:10.1021/ja029267j
- Nasrollahzadeh M, Sajjadi M, Sajadi SM. Green synthesis of Cu/zirconium silicate nanocomposite by using rubia tinctorum leaf extract and its application in the preparation of N-benzyl-N-arylcyanamides. *Appl Organomet Chem.* 2019;33(2):e4705.
- Ismail M, Gul S, Khan MI, et al. Green synthesis of zerovalent copper nanoparticles for efficient reduction of toxic azo dyes congo red and methyl orange. *Green Process Synth.* 2019;8(1):135–143. doi:10.1515/gps-2018-0038
- Wang C, Ciganda R, Salmon L, et al. Highly efficient transition metal nanoparticle catalysts in aqueous solutions. *Angew Chem Int Ed.* 2016;55(9):3091–3095. doi:10.1002/anie.201511305
- Sun J, Fujita S-I, Arai M. Development in the green synthesis of cyclic carbonate from carbon dioxide using ionic liquids. *J Organomet Chem.* 2005;690(15):3490–3497. doi:10.1016/j.jorganchem.2005.02.011
- Mehta A, Mishra A, Basu S, et al. Band gap tuning and surface modification of carbon dots for sustainable environmental remediation and photocatalytic hydrogen production – a review. *J Environ Manage.* 2019;250:109486. doi:10.1016/j.jenvman.2019.109486
- Reddy NR, Bhargav U, Kumari MM, et al. Highly efficient solar light-driven photocatalytic hydrogen production over Cu/FCNTs-titania quantum dots-based heterostructures. *J Environ Manage.* 2020;254:109747. doi:10.1016/j.jenvman.2019.109747
- Reddy CV, Reddy IN, Harish VVN, et al. Efficient removal of toxic organic dyes and photoelectrochemical properties of iron-doped zirconia nanoparticles. *Chemosphere.* 2020;239:124766. doi:10.1016/j.chemosphere.2019.124766
- Reddy NL, Rao VN, Vijayakumar M, et al. A review on frontiers in plasmonic nano-photocatalysts for hydrogen production. *Int J Hydrogen Energy.* 2019;44(21):10453–10472. doi:10.1016/j.ijhydene.2019.02.120
- Reddy CV, Reddy IN, Akkinepally B, et al. Synthesis and photoelectrochemical water oxidation of (Y, Cu) codoped α-Fe<sub>2</sub>O<sub>3</sub> nanostructure photoanode. *J Alloys Compd.* 2020;814:152349. doi:10.1016/j.jallcom.2019.152349
- Rao VN, Lakshmana Reddy N, Mamatha Kumari M, et al. Photocatalytic recovery of H<sub>2</sub> from H<sub>2</sub>S containing wastewater: surface and interface control of photo-excitons in Cu<sub>2</sub>S@TiO<sub>2</sub> core-shell nanostructures. *Appl Catal B.* 2019;254:174–185. doi:10.1016/j.apcatb.2019.04.090
- Reddy CV, Reddy IN, Reddy KR, et al. Template-free synthesis of tetragonal Co-doped ZrO<sub>2</sub> nanoparticles for applications in electrochemical energy storage and water treatment. *Electrochim Acta.* 2019;317:416–426. doi:10.1016/j.electacta.2019.06.010
- Candan F, Unlu M, Tepe B, et al. Antioxidant and antimicrobial activity of the essential oil and methanol extracts of Achillea millefolium subsp. millefolium Afan. (Asteraceae). *J Ethnopharmacol.* 2003;87(2–3):215–220. doi:10.1016/S0378-8741(03)00149-1
- Afsharypour S, Asgary S, Lockwood G. Volatile constituents of Achillea millefolium L. ssp. millefolium from Iran. *Flavour Fragr J.* 1996;11(5):265–267. doi:10.1002/(SICI)1099-1026(199609)11:5<265::AID-FFJ592>3.0.CO;2-F
- Hachey J-M, Collin G-J, Gagnon M-J, et al. Extraction and GC/MS analysis of the essential oil of Achillea millefolium L. complex (compositae). *J Essent Oil Res.* 1990;2(6):317–326. doi:10.1080/10412905.1990.9697890
- Moussaoui AE, Jawhari FZ, Almehdi AM, et al. Antibacterial, antifungal and antioxidant activity of total polyphenols of Withania frutescens. L. *Bioorg Chem.* 2019;93:103337. doi:10.1016/j.bioorg.2019.103337
- Fowsiya J, Madhumitha G, Al-Dhabi NA, et al. Photocatalytic degradation of Congo red using Carissa edulis extract capped zinc oxide nanoparticles. *J Photochem Photobiol B.* 2016;162:395–401. doi:10.1016/j.jphotobiol.2016.07.011
- Iqbal J, Shah NS, Sayed M, et al. Deep eutectic solvent-mediated synthesis of ceria nanoparticles with the enhanced yield for photocatalytic degradation of flumequine under UV-C. *J Water Process Eng.* 2020;33:101012. doi:10.1016/j.jwpe.2019.101012

27. Alves D, Santos CG, Paixão MW, et al. CuO nanoparticles: an efficient and recyclable catalyst for cross-coupling reactions of organic diselenides with aryl boronic acids. *Tetrahedron Lett.* 2009;50(48):6635–6638. doi:10.1016/j.tetlet.2009.09.052
28. Chaudhary GR, Bansal P, Kaur N, et al. Recyclable CuO nanoparticles as heterogeneous catalysts for the synthesis of xanthenes under solvent free conditions. *RSC Adv.* 2014;4(90):49462–49470. doi:10.1039/C4RA07620F
29. Deol H, Pramanik S, Kumar M, et al. Supramolecular ensemble of a TICT-AIEE active pyrazine derivative and CuO NPs: a potential photocatalytic system for sonogashira couplings. *ACS Catal.* 2016;6(6):3771–3783. doi:10.1021/acscatal.6b00393
30. Rabiee N, Bagherzadeh M, Kiani M, et al. Rosmarinus officinalis directed palladium nanoparticle synthesis: investigation of potential anti-bacterial, anti-fungal and Mizoroki-Heck catalytic activities. *Adv Powder Technol.* 2020. doi:10.1016/j.apt.2020.01.024
31. Bagherzadeh M, Bayrami A, Kia R, et al. Two new copper (II) complexes with chelating N, O-type bidentate ligands: synthesis, characterization, crystal structure and catalytic activity in azide-alkyne cycloaddition reaction. *Inorganica Chim Acta.* 2017;466:398–404. doi:10.1016/j.ica.2017.06.046
32. Veisi H, Mohammadi L, Hemmati S, et al. In situ immobilized silver nanoparticles on rubia tinctorum extract-coated ultrasmall iron oxide nanoparticles: an efficient nanocatalyst with magnetic recyclability for synthesis of propargylamines by A3 coupling reaction. *ACS Omega.* 2019;4(9):13991–14003. doi:10.1021/acsomega.9b01720
33. GhavamiNejad A, Kalantarifard A, Yang GS, et al. In-situ immobilization of silver nanoparticles on ZSM-5 type zeolite by catechol redox chemistry, a green catalyst for A3-coupling reaction. *Micropor Mesopor Mat.* 2016;225:296–302. doi:10.1016/j.micromeso.2015.12.050
34. Terra JC, Moores A, Moura FC. Amine-functionalized mesoporous silica as a support for on-demand release of copper in the A3-coupling reaction: ultralow concentration catalysis and confinement effect. *ACS Sustain Chem Eng.* 2019;7(9):8696–8705. doi:10.1021/acssuschemeng.9b00576
35. Bagherzadeh M, Kaveh R, Ozkar S, et al. Preparation and characterization of a new CdS–NiFe 2 O 4/reduced graphene oxide photocatalyst and its use for degradation of methylene blue under visible light irradiation. *Res Chem Intermed.* 2018;44(10):5953–5979. doi:10.1007/s11164-018-3466-1
36. Raja A, Ashokkumar S, Pavithra Marthandam R, et al. Eco-friendly preparation of zinc oxide nanoparticles using Tabernaemontana divaricata and its photocatalytic and antimicrobial activity. *J Photochem Photobiol B.* 2018;181:53–58. doi:10.1016/j.jphotobiol.2018.02.011
37. Karthik K, Dhanuskodi S, Gobinath C, et al. Multifunctional properties of microwave assisted CdO–NiO–ZnO mixed metal oxide nanocomposite: enhanced photocatalytic and antibacterial activities. *J Mater Sci Mater Electron.* 2018;29(7):5459–5471.
38. Samu GF, Veres Á, Tallósy SP, et al. Photocatalytic, photoelectrochemical, and antibacterial activity of benign-by-design mechanocchemically synthesized metal oxide nanomaterials. *Catal Today.* 2017;284:3–10. doi:10.1016/j.cattod.2016.07.010
39. Siddiqui MA, Alhadlaq HA, Ahmad J, et al. Copper oxide nanoparticles induced mitochondria mediated apoptosis in human hepatocarcinoma cells. *PLoS One.* 2013;8(8):e69534. doi:10.1371/journal.pone.0069534
40. Sharma V, Anderson D, Dhawan A. Zinc oxide nanoparticles induce oxidative DNA damage and ROS-triggered mitochondria mediated apoptosis in human liver cells (HepG2). *Apoptosis.* 2012;17(8):852–870. doi:10.1007/s10495-012-0705-6
41. Lu X, Tai Y-J, Chiang C-H, et al. In vitro cytotoxicity and induction of apoptosis by silica nanoparticles in human HepG2 hepatoma cells. *Int J Nanomedicine.* 2011;6:1889. doi:10.2147/IJN.S25646
42. Li Y, Guo M, Lin Z, et al. Polyethylenimine-functionalized silver nanoparticle-based co-delivery of paclitaxel to induce HepG2 cell apoptosis. *Int J Nanomedicine.* 2016;11:6693. doi:10.2147/IJN.S122666
43. Kumar PPNV, Shameem U, Kollu P, et al. Green synthesis of copper oxide nanoparticles using Aloe vera leaf extract and its antibacterial activity against fish bacterial pathogens. *BioNanoScience.* 2015;5(3):135–139. doi:10.1007/s12668-015-0171-z
44. Sharma JK, Akhtar MS, Ameen S, et al. Green synthesis of CuO nanoparticles with leaf extract of Calotropis gigantea and its dye-sensitized solar cells applications. *J Alloys Compd.* 2015;632:321–325. doi:10.1016/j.jallcom.2015.01.172
45. Duman F, Ocsay I, Kup FO. Chamomile flower extract-directed CuO nanoparticle formation for its antioxidant and DNA cleavage properties. *Mater Sci Eng C.* 2016;60:333–338. doi:10.1016/j.msec.2015.11.052
46. Dutta B, Kar E, Bose N, et al. Significant enhancement of the electroactive  $\beta$ -phase of PVDF by incorporating hydrothermally synthesized copper oxide nanoparticles. *RSC Adv.* 2015;5(127):105422–105434. doi:10.1039/C5RA21903E
47. Ghorbani HR, Fazeli I, Fallahi AA. Biosynthesis of copper oxide nanoparticles using extract of E. coli. *Orient J Chem.* 2015;31(1):515–517. doi:10.13005/ojc/310165
48. Berra D, Laouini SE, Benhaoua B, Ouahrani MR, Berrani D, Rahal A. Green synthesis of copper oxide nanoparticles by phoenix dactylifera l leaves extract. *Dig J Nanomater Bios.* 2018;13(4):1231–1238.
49. Saif S, Tahir A, Asim T, et al. Plant mediated green synthesis of CuO nanoparticles: comparison of toxicity of engineered and plant mediated CuO nanoparticles towards Daphnia magna. *Nanomaterials.* 2016;6(11):205. doi:10.3390/nano6110205
50. Pakzad K, Alinezhad H, Nasrollahzadeh M. Green synthesis of Ni@Fe3O4 and CuO nanoparticles using Euphorbia maculata extract as photocatalysts for the degradation of organic pollutants under UV-irradiation. *Ceram Int.* 2019;45(14):17173–17182. doi:10.1016/j.ceramint.2019.05.272
51. Selvan SM, Vijai Anand K, Govindaraju K, et al. Green synthesis of copper oxide nanoparticles and mosquito larvicidal activity against dengue, Zika and chikungunya causing vector Aedes aegypti. *IET Nanobiotechnol.* 2018;12(8):1042–1046. doi:10.1049/iet-nbt.2018.5083
52. Khatami M, Heli H, Mohammadzadeh Jahani P, et al. Copper/copper oxide nanoparticles synthesis using Stachys lavandulifolia and its antibacterial activity. *IET Nanobiotechnol.* 2017;11(6):709–713. doi:10.1049/iet-nbt.2016.0189
53. Sivaraj R, Rahman PKSM, Rajiv P, et al. Biogenic copper oxide nanoparticles synthesis using Tabernaemontana divaricata leaf extract and its antibacterial activity against urinary tract pathogen. *Spectrochim Acta A Mol Biomol Spectrosc.* 2014;133:178–181. doi:10.1016/j.saa.2014.05.048
54. Sankar R, Manikandan P, Malarvizhi V, et al. Green synthesis of colloidal copper oxide nanoparticles using Carica papaya and its application in photocatalytic dye degradation. *Spectrochim Acta A Mol Biomol Spectrosc.* 2014;121:746–750. doi:10.1016/j.saa.2013.12.020
55. Nagar N, Devra V. Green synthesis and characterization of copper nanoparticles using Azadirachta indica leaves. *Mater Chem Phys.* 2018;213:44–51. doi:10.1016/j.matchemphys.2018.04.007
56. Bagherzadeh M, Mahmoudi H, Ataie S, et al. Synthesis, characterization, and comparison of two new copper(II) complexes containing Schiff-base and diazo ligands as new catalysts in CuAAC reaction. *Inorganica Chim Acta.* 2019;492:213–220. doi:10.1016/j.ica.2019.04.036
57. Reddy KR, Rajgopal K, Kantam ML. Copper (II)-promoted regioselective synthesis of 1, 4-disubstituted 1, 2, 3-triazoles in water. *Synlett.* 2006;2006(06):957–959. doi:10.1055/s-2006-933134
58. Nador F, Volpe MA, Alonso F, et al. Copper nanoparticles supported on silica coated maghemite as versatile, magnetically recoverable and reusable catalyst for alkyne coupling and cycloaddition reactions. *Appl Catal a Gen.* 2013;455:39–45. doi:10.1016/j.apcata.2013.01.023
59. Wang C, Yang F, Cao Y, et al. Cupric oxide nanowires on three-dimensional copper foam for application in click reaction. *RSC Adv.* 2017;7(16):9567–9572. doi:10.1039/C7RA00014F

60. Kim A, Muthuchamy N, Yoon C, et al. MOF-derived Cu@ Cu<sub>2</sub>O nanocatalyst for oxygen reduction reaction and cycloaddition reaction. *Nanomaterials*. 2018;8(3):138. doi:10.3390/nano8030138
61. Li Y, Zhang W, Niu J, et al. Mechanism of photogenerated reactive oxygen species and correlation with the antibacterial properties of engineered metal-oxide nanoparticles. *ACS Nano*. 2012;6(6):5164–5173. doi:10.1021/nm300934k
62. Raghupathi KR, Koodali RT, Manna AC. Size-dependent bacterial growth inhibition and mechanism of antibacterial activity of zinc oxide nanoparticles. *Langmuir*. 2011;27(7):4020–4028. doi:10.1021/la104825u
63. Apperlot G, Lellouche J, Lipovsky A, et al. Understanding the antibacterial mechanism of CuO nanoparticles: revealing the route of induced oxidative stress. *Small*. 2012;8(21):3326–3337. doi:10.1002/sml.201200772
64. Dizaj SM, Lotfipour F, Barzegar-Jalali M, et al. Antimicrobial activity of the metals and metal oxide nanoparticles. *Mater Sci Eng C*. 2014;44:278–284. doi:10.1016/j.msec.2014.08.031
65. Misra A, Jain S, Kishore D, et al. A facile one pot synthesis of novel pyrimidine derivatives of 1, 5-benzodiazepines via domino reaction and their antibacterial evaluation. *J Microbiol Methods*. 2019;163:105648. doi:10.1016/j.mimet.2019.105648
66. Sharma P, Pant S, Dave V, et al. Green synthesis and characterization of copper nanoparticles by *Tinospora cardifolia* to produce nature-friendly copper nano-coated fabric and their antimicrobial evaluation. *J Microbiol Methods*. 2019;160:107–116. doi:10.1016/j.mimet.2019.03.007
67. Nagaraja A, Jalageri MD, Puttaiahgowda YM, et al. A review on various maleic anhydride antimicrobial polymers. *J Microbiol Methods*. 2019;163:105650. doi:10.1016/j.mimet.2019.105650
68. Cioffi N, Torsi L, Ditaranto N, et al. Copper nanoparticle/polymer composites with antifungal and bacteriostatic properties. *Chem Mater*. 2005;17(21):5255–5262. doi:10.1021/cm0505244
69. Ingle AP, Duran N, Rai M. Bioactivity, mechanism of action, and cytotoxicity of copper-based nanoparticles: a review. *Appl Microbiol Biotechnol*. 2014;98(3):1001–1009. doi:10.1007/s00253-013-5422-8
70. Weitz IS, Maoz M, Panitz D, et al. Combination of CuO nanoparticles and fluconazole: preparation, characterization, and antifungal activity against *Candida albicans*. *J Nanopart Res*. 2015;17(8):342. doi:10.1007/s11051-015-3149-4
71. Ivask A, Juganson K, Bondarenko O, et al. Mechanisms of toxic action of Ag, ZnO and CuO nanoparticles to selected ecotoxicological test organisms and mammalian cells in vitro: a comparative review. *Nanotoxicology*. 2014;8(sup1):57–71. doi:10.3109/17435390.2013.855831
72. Piret J-P, Jacques D, Audinot J-N, et al. Copper(ii) oxide nanoparticles penetrate into HepG2 cells, exert cytotoxicity via oxidative stress and induce pro-inflammatory response. *Nanoscale*. 2012;4(22):7168–7184. doi:10.1039/c2nr31785k
73. Kung M-L, Hsieh S-L, Wu -C-C, et al. Enhanced reactive oxygen species overexpression by CuO nanoparticles in poorly differentiated hepatocellular carcinoma cells. *Nanoscale*. 2015;7(5):1820–1829. doi:10.1039/C4NR05843G
74. Zhang Y, Xu Y, Xi X, et al. Amino acid-modified chitosan nanoparticles for Cu<sup>2+</sup> chelation to suppress CuO nanoparticle cytotoxicity. *J Mater Chem B*. 2017;5(19):3521–3530. doi:10.1039/C7TB00344G

## International Journal of Nanomedicine

### Publish your work in this journal

The International Journal of Nanomedicine is an international, peer-reviewed journal focusing on the application of nanotechnology in diagnostics, therapeutics, and drug delivery systems throughout the biomedical field. This journal is indexed on PubMed Central, MedLine, CAS, SciSearch®, Current Contents®/Clinical Medicine,

Journal Citation Reports/Science Edition, EMBase, Scopus and the Elsevier Bibliographic databases. The manuscript management system is completely online and includes a very quick and fair peer-review system, which is all easy to use. Visit <http://www.dovepress.com/testimonials.php> to read real quotes from published authors.

Submit your manuscript here: <https://www.dovepress.com/international-journal-of-nanomedicine-journal>

Dovepress